IEEE Access
Multidisciplinary | Rapid Review | Open Access Journal

Received February 3, 2020, accepted February 21, 2020, date of publication February 27, 2020, date of current version March 10, 2020.

Digital Object Identifier 10.1109/ACCESS.2020.2976705

Bandwidth-Enhanced Circularly Polarized Spiral Antenna With Compact Size

LING-LU CHEN, LEI CHANG, ZHUANG-ZHI CHEN, AND QIAO-NA QIU
No. 36 Research Institute, CETC, Jiaxing 314033, China

Corresponding author: Lei Chang (yutian_1986@163.com)

This work was supported by the Young Elite Scientists Sponsorship Program by China Association for Science and Technology (CAST) under Grant 2017QNRC001.

ABSTRACT A compact circularly polarized (CP) spiral antenna with enhanced impedance and 3-dB axial ratio (AR) bandwidths that is fed by a tapered coax balun is presented. The antenna is composed of a two-arm nonself-complementarity planar equiangular spiral, a z-directional helix, absorbing material with a stepped cylindrical honeycomb structure, and a ground plane. The z-directional helix is used to extend the current path and to improve the impedance matching and AR in the low-frequency band. The coupling between the nonself-complementarity planar spiral arms is increased, which improves the impedance matching in the low-frequency band and the AR at approximately 5.55 GHz. The stepped cylindrical absorbing material can reduce the reverse current and improve the AR in the high-frequency band. The measured results show that the impedance bandwidth and 3-dB AR bandwidths range from 0.5 to 6 GHz and from 0.5 to 5.8 GHz, respectively. The overall size of the proposed antenna is $0.189\lambda_L \times 0.065\lambda_L$ (diameter $\times$ height, where λ_L is the free-space wavelength at the starting frequency).

INDEX TERMS Spiral antenna, absorbing material, ultrawideband, miniaturization.

I. INTRODUCTION

Wideband antennas have attracted widespread attention for application in many communication and radar systems. For a wideband wireless system requiring circularly polarized (CP) radiation characteristics, a spiral antenna is a good choice. Many techniques have been adopted for wideband CP spiral antenna designs. In [1], a polygonal-modified Archimedean spiral with a bandwidth of 2-18 GHz was studied. An Archimedean spiral antenna operating from 2 to over 20 GHz and fed by a stripline was presented in [2]. A wideband CP equiangular spiral antenna with a 3-dB axial ratio (AR) bandwidth of 3-14.5 GHz that was fed by an integrated balun was proposed in [3]. In [4], by using chip resistors inside the substrate, a planar equiangular spiral antenna achieved an impedance bandwidth of 2-18 GHz. A two-arm Archimedean spiral with a stepped ground plane cavity operating in the frequency band of 2-10 GHz was designed as a feed for a parabolic reflector [5]. An equiangular spiral antenna using a ring-shaped absorbing strip that operates in the frequency band of 3-10 GHz was studied in [6]. A two-arm Archimedean spiral antenna fed by a Dyson balun operating in the frequency band of 18-110 GHz was studied in [7]. In [8], a single-arm spiral antenna with a disc plane and a ring-shaped absorbing material was proposed; the antenna operates from 3 GHz to 10 GHz. A spiral antenna fed by a coplanar waveguide (CPW) achieved a frequency band of 11.4-17.5 GHz in [9]. By using a frequency selective surface (FSS), an Archimedean spiral antenna was designed to improve the front-to-back (F/B) ratio and gain in the frequency band of 3-10 GHz [10].

Recently, compact spiral antennas have been required more frequently for limited-space systems. Research regarding compact spiral antennas has attracted much attention. Some wideband compact spiral antennas were presented in [11]–[19]. In [11], metallic posts were employed to achieve bandwidth enhancement and a low-profile ($0.1\lambda_L$) for an equiangular spiral antenna; the posts were placed between the planar spiral and metal reflector. A sine wave meander line was introduced to a planar Archimedean spiral antenna to reduce the aperture area [12]. The 3-dB AR bandwidth was from 1.63 to 10 GHz, and the overall size of the antenna was $0.348\lambda_{1.63\ \mathrm{GHz}} \times 0.206\lambda_{1.63\ \mathrm{GHz}}$ (diameter $\times$ height). In [13], a spiral antenna using a semifractal reflector and a combination of the equiangular Archimedean lines and a meander line was designed to obtain a 3-dB AR bandwidth of 0.9-4.37 GHz. The overall size of the antenna was $0.3\lambda_{0.9\ \mathrm{GHz}} \times 0.3\lambda_{0.9\ \mathrm{GHz}} \times 0.15\lambda_{0.9\ \mathrm{GHz}}$. To achieve 3-D

The associate editor coordinating the review of this manuscript and approving it for publication was Haiwen Liu.

miniaturization, a combination of z-directed meandering and a tapered substrate profile was applied [14]. The impedance bandwidth was from 0.8 to 3 GHz. However, in the whole frequency band, the AR of most frequencies was greater than 3 dB. The overall size of the antenna was $0.203\lambda_{0.8\ \mathrm{GHz}} \times 0.102\lambda_{0.8\ \mathrm{GHz}}$ (diameter × height). In [15], different high impedance surface (HIS) sections were applied to an Archimedean spiral antenna. This antenna operated from 3 to 10 GHz with a height of $0.085\lambda_L$. A low-profile equiangular spiral antenna with an electromagnetic band gap (EBG) reflector was presented in [16]; the antenna operated from 3 to 10 GHz. The height of the antenna was $0.07\lambda_L$. However, in the frequency bands of approximately 3-3.8 GHz and 5-5.4 GHz, the AR was greater than 3 dB. In [17], a spiral antenna printed on an extremely thin magnetodielectric substrate was presented. The antenna achieved an operating bandwidth of 300-1000 MHz and a very small height of $0.061\lambda_L$. The aperture size of the antenna was $0.4\lambda_L \times 0.4\lambda_L$. A differential-fed Archimedean spiral with a novel loading structure and a ring-shaped absorber was studied to achieve miniaturization design with an overall size of $0.21\lambda_L \times 0.21\lambda_L \times 0.09\lambda_L$ [18]. This antenna operated from 0.5 to 1.4 GHz. In [19], in order to reduce the size of an Archimedean spiral antenna, two arms were extended on the profile and connected together at the end. Furthermore, four lumped resistors were used to improve the performance of the low frequency band. The 3-dB AR bandwidth was from 2 to 6 GHz, and the overall size of the antenna was $0.24\lambda_{2\ \mathrm{GHz}} \times 0.24\lambda_{2\ \mathrm{GHz}} \times 0.13\lambda_{2\ \mathrm{GHz}}$.

In this paper, a miniaturization method for CP spiral antennas is proposed. The z-directional helix increases the current path, which improves the impedance matching and AR in the low-frequency band. Nonself-complementarity planar spiral arms are used to improve the impedance matching in the low-frequency band and the AR at approximately 5.55 GHz. To further improve the AR bandwidth, stepped cylindrical absorbing material is applied to reduce the reverse current in the high-frequency band, thereby reducing the cross polarization. Lumped resistor loading is not required. By applying the proposed method, the antenna achieves a 169.2% impedance bandwidth for VSWR ≤ 2 and a 168.3% 3-dB AR bandwidth; moreover, the antenna is miniaturized in three dimensions. The size of the proposed antenna can be reduced to $0.189\lambda_L \times 0.065\lambda_L$ (diameter × height). A prototype of the proposed antenna is fabricated. The design procedure of the proposed antenna, the simulated and measured results are presented and discussed.

II. ANTENNA DESIGN

The proposed spiral antenna consists of a planar equiangular spiral, a z-directional helix, an absorbing material, a tapered coax balun and a ground plane; it is depicted in Fig. 1. The planar spiral and z-directional helix are printed on substrates with relative dielectric constant $\varepsilon_r = 2.5$, loss tangent $\tan\delta = 0.0018$, and thicknesses of 2 mm and 0.127 mm, respectively. The radius of the planar spiral is *rsub*. The z-directional helix

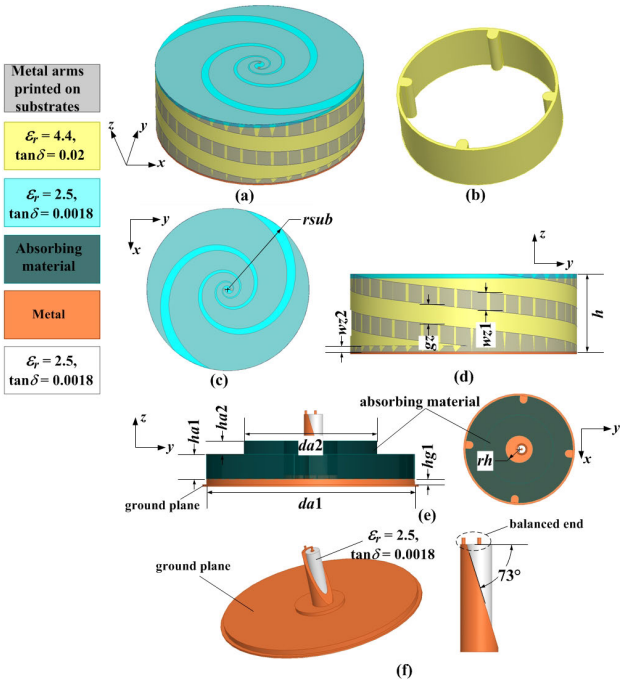

FIGURE 1. Geometry of the proposed spiral antenna. (a) 3-D view, (b) detailed view of hollow cylinder, (c) top view, (d) side view, (e) detailed view of the interior of the antenna, and (f) coax balun.

printed on a substrate is wound around the hollow cylinder with a relative dielectric constant of 4.4, a loss tangent of 0.02, and a thickness of 2 mm. Four columns are added to the hollow cylinder to support the planar spiral. The height of z-directional helix is h. A metal ring with width $wz2$ is used to connect the ends of the z-directional helix.

The feed balun is based on a coaxial line. The diameters of the central core and the dielectric material of the coaxial line are 2.2 mm and 8 mm, respectively. The electromagnetic parameters of the dielectric material are $\varepsilon_r = 2.5$ and $\tan\delta = 0.0018$. Upon moving toward the balanced end, the metallic shield slot of the coaxial line opens. This balun changes the unbalanced coaxial line to a balanced twin line and yields the impedance transformation. In our design, a modified nonself-complementarity spiral is proposed; it is obtained by rotating the traditional self-complementarity spiral $\pm rota$ around the z-axis, as shown in Fig. 2. The traditional self-complementarity spiral is defined by

$$r_1 = r_0 e^{a\phi}, \quad 0^\circ \leq \phi \leq 360^\circ \times 2.05 - \delta \tag{1}$$

$$r_2 = r_0 e^{a(\phi-\delta)}, \quad 0^\circ \leq \phi \leq 360^\circ \times 2.05 \tag{2}$$

where $r_0 = 3$ mm, $a = 0.26$, and $\delta = 90^\circ$. Table 1 reports the optimized dimensions of the antenna.

III. ANTENNA OPERATION PRINCIPLE

The influences of the nonself-complementarity planar equiangular spiral, the z-directional helix, and the stepped cylindrical absorbing material are studied to illustrate the design process of the proposed antenna.

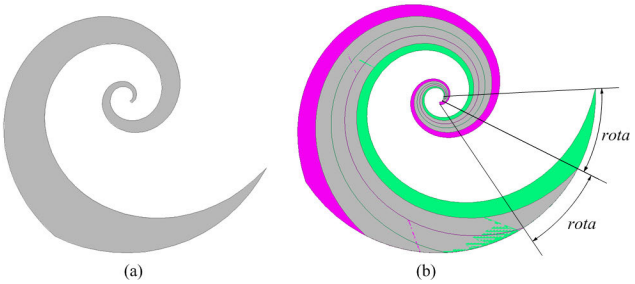

FIGURE 2. Arm of planar equiangular spiral: (a) traditional self-complementarity spiral and (b) modified nonself-complementarity spiral.

TABLE 1. Dimensions of the proposed antenna.

Parameters	Values	Parameters	Values
rsub	56.8 mm	*h*	39 mm
gz	9.85 mm	*wz*1	9 mm
*wz*2	3 mm	*ha*1	13 mm
*ha*2	7 mm	*da*1	109.6 mm
*da*2	70 mm	*hg*1	3 mm
rota	30°	*rh*	28 mm

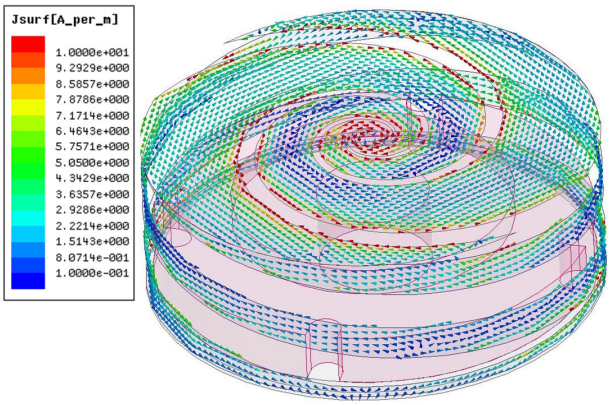

FIGURE 3. Current distributions of the antenna at 0.5 GHz.

A. EFFECT OF THE Z-DIRECTIONAL HELIX

Fig. 3 shows the current distributions of the proposed antenna at 0.5 GHz. It can be observed that the currents on the z-directional helix and the planar spiral are in the same direction. This result means that the z-directional helix extends the current path in the low-frequency band.

The effects of the z-directional helix on the impedance matching, AR and gain are shown in Fig. 4. When the z-directional helix is removed, the impedance bandwidth is narrow with 1.11-6 GHz for VSWR ≤ 2. Meanwhile, the gain decreases from 0.5 to 2 GHz, and the AR is greater than 3 dB from 0.5 to 2.05 GHz.

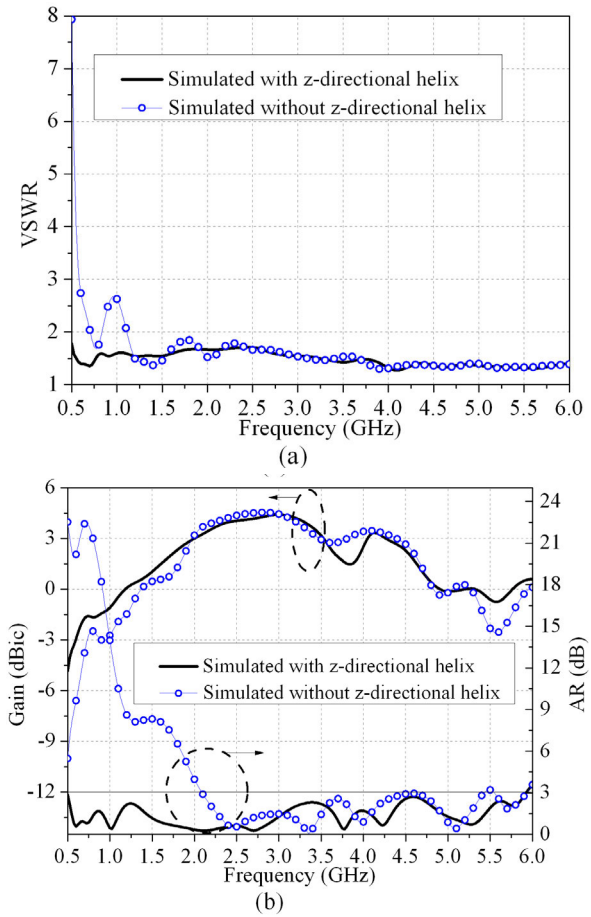

FIGURE 4. Effects of the z-directional helix. (a) VSWR and (b) broadside gain and AR.

B. EFFECT OF THE NONSELF-COMPLEMENTARITY SPIRAL

We studied the effect of the nonself-complementarity spiral on the antenna performance. Fig. 5 shows comparisons of the simulated results for the antennas with a self-complementarity spiral and those with a modified nonself-complementarity spiral. By introducing the nonself- complementarity spiral, the impedance matching in the band of 0.5-1.33 GHz and the AR in the band of 5.44-5.71 GHz are improved. We can see that a wide impedance bandwidth of 0.5-6 GHz for VSWR $\leq$ 2 and a 3-dB AR bandwidth of 0.5-5.925 GHz were obtained. However, the gain from 3 to 6 GHz is decreased when the nonself- complementarity spiral is used.

Fig. 6 shows the current distributions of the nonself- complementarity and self-complementarity spirals at 0.5 GHz. The currents at the edge of the nonself-complementarity spiral are increased, and more energy is radiated. The input impedance of the antennas using the nonself-complementarity and self-complementarity spirals is shown in Fig. 7. The input resistance and reactance of the antenna using the nonself-complementarity spiral is increased, and the impedance matching in the low-frequency band is improved.

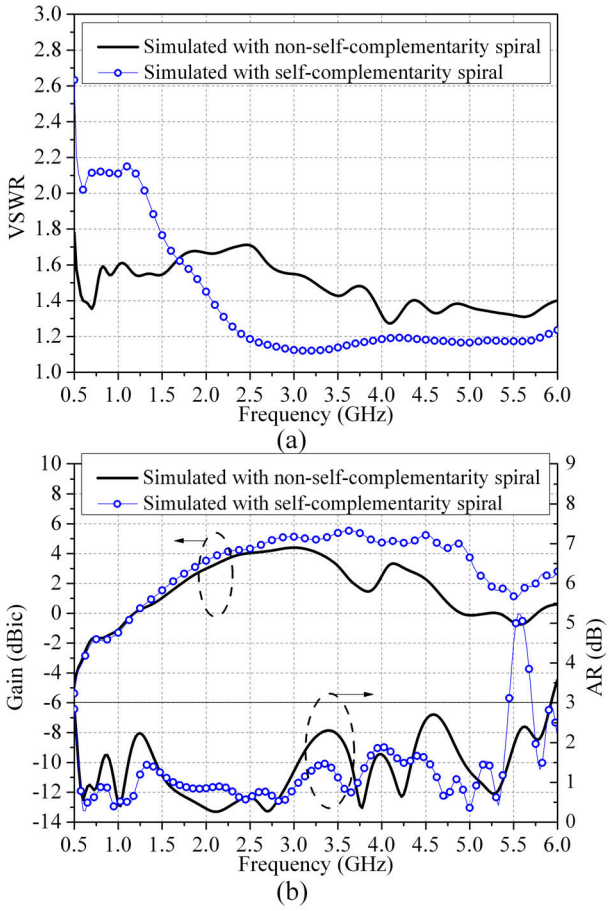

FIGURE 5. Comparisons of simulated results. (a) VSWR and (b) broadside gain and AR.

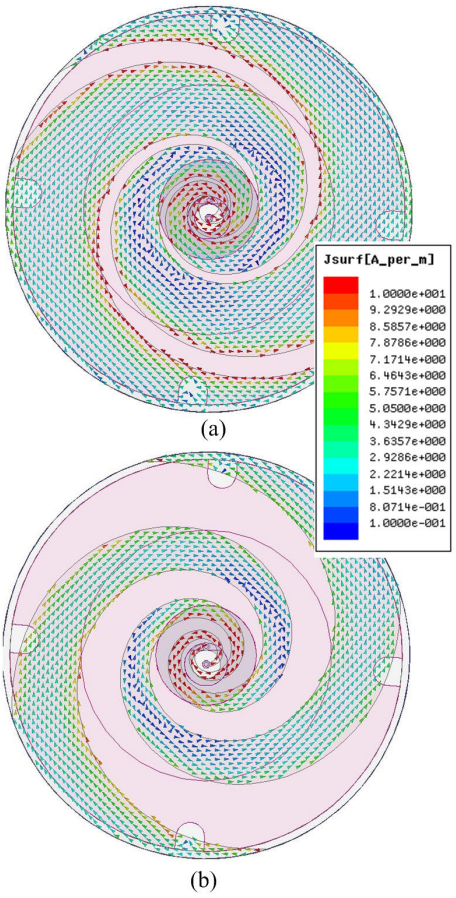

FIGURE 6. Current distributions of the planar spirals at 0.5 GHz. (a) Nonself-complementarity spiral and (b) self-complementarity spiral.

The AR of the antenna using the self-complementarity spiral at approximately 5.5 GHz gets worse, as shown in Fig. 5. This is due to the reverse currents generated on the self-complementarity spiral (shown in Fig. 8(b)), and the increase in cross polarization. When the nonself-complementarity spiral is used, the coupling between the two spiral arms is enhanced. As the reverse currents are generated on the arm, the opposite currents are coupled to the other arm and these two currents cancel each other out. The cross polarization of the antenna is reduced. This allows the antenna using the nonself-complementarity spiral to have a good CP radiation performance. Furthermore, the gain is decreased due to the opposite currents coupled to the other arm.

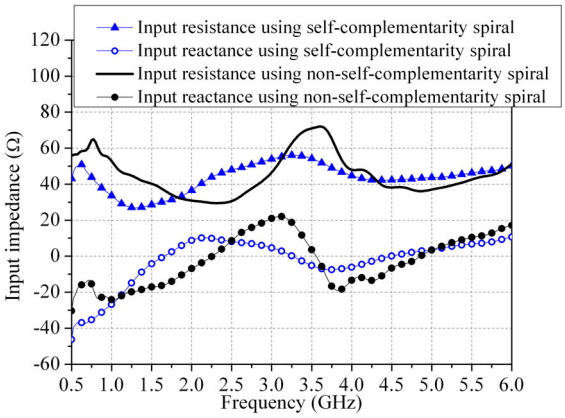

FIGURE 7. Input impedance of the antennas using nonself-complementarity and self- complementarity spirals.

C. EFFECT OF THE STEPPED CYLINDRICAL ABSORB-ING MATERIAL

To investigate the effects of the absorbing material with a stepped cylindrical honeycomb structure, several simulation calculations were performed with different values of $da2$ and $ha2$, as shown in Fig. 9. When $da2 = 70$ mm, $ha2 = 0$ mm and $da2 = da1 = 109.6$ mm, $ha2 = 7$ mm, the stepped cylindrical absorbing material becomes a traditional ring-shaped absorbing material. When the thickness of the traditional ring-shaped absorbing material is only $ha1$ ($ha2 = 0$ mm), the impedance matching in the low-frequency band becomes worse, and the gain decreases in the high-frequency band; moreover, the AR is greater than 3 dB at both low and high frequencies. When the thickness of the traditional ring-shaped absorbing material is $ha1 + ha2$, the VSWR changes

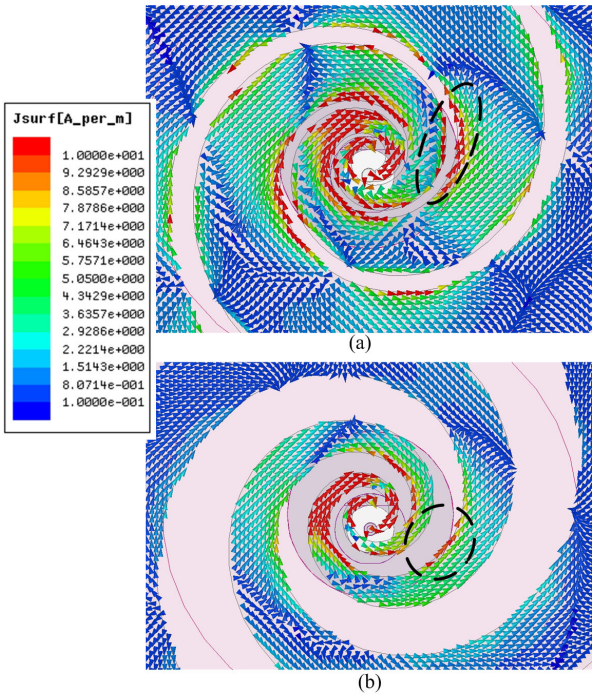

FIGURE 8. Current distributions of the planar spirals at 5.55 GHz. (a) Nonself-complementarity spiral and (b) self-complementarity spiral.

very little and the gain decreases in the low-frequency band. Meanwhile, the AR is improved in the low-frequency band, but it is greater than 3 dB in the band of 5.59-5.925 GHz. It can be observed that the stepped cylindrical absorbing material has an obvious influence on the VSWR, gain and AR.

When the ring-shaped absorbing material with $da2 = 70$ mm, $ha2 = 0$ mm is used, the thickness of the absorbing material in the middle area is reduced, and the absorption capacity of the reverse currents decreases, leading to the deterioration of the AR, as shown in Fig. 10.

By using the stepped cylindrical absorbing material with $da2 = 70$ mm, $ha2 = 7$ mm, the reverse currents are reduced compared to those produced when the ring-shaped absorbing material with $da2 = da1 = 109.6$ mm, $ha2 = 7$ mm is used, as shown in Fig. 11. Then, the AR is improved in the high-frequency band. The ring-shaped absorbing material with $da2 = da1 = 109.6$ mm, $ha2 = 7$ mm at the edge of the antenna is thicker than the stepped cylindrical absorbing material, and this reduces the gain in the low-frequency band.

To further illustrate the effects of the stepped cylindrical absorbing material, the simulated results for the antenna with and without the absorbing material are shown in Fig. 12. By introducing the absorbing material, the impedance matching especially in the low-frequency band, is improved, and the AR performance is improved in the whole operating band. Moreover, the unidirectional radiation performance is improved in the 3.6-4.5 GHz and 5.65-6 GHz bands. Nevertheless, the radiation efficiency is significantly

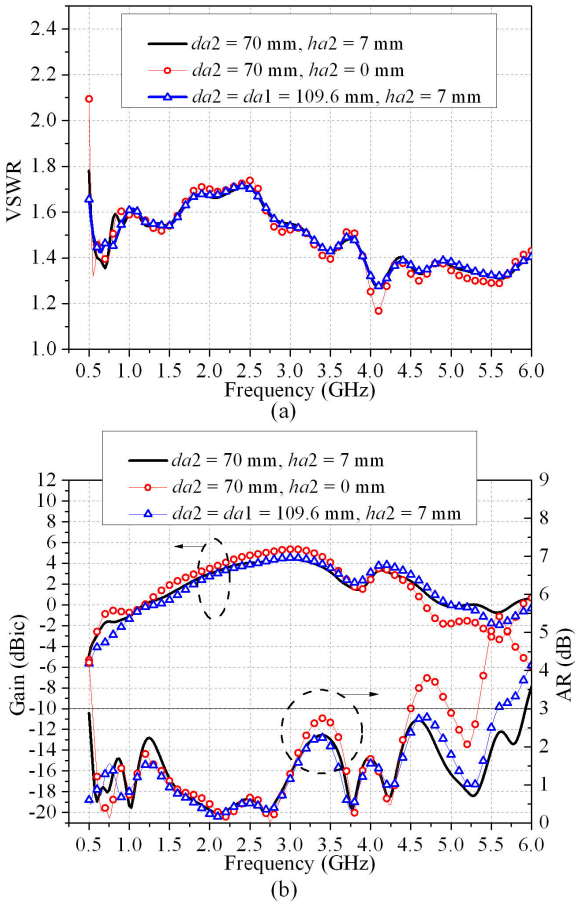

FIGURE 9. Effects of the absorbing material. (a) VSWR and (b) broadside gain and AR.

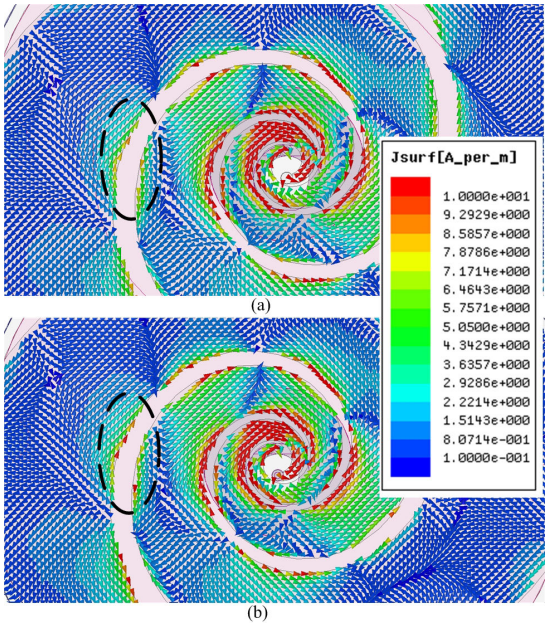

FIGURE 10. Current distributions of the antennas using (a) stepped cylindrical absorbing material and (b) ring-shaped absorbing material with $da2 = 70$ mm, $ha2 = 0$ mm at 5.6 GHz.

decreased when the absorbing material is used. In the low-frequency band, the radiation efficiency of the antenna is low,

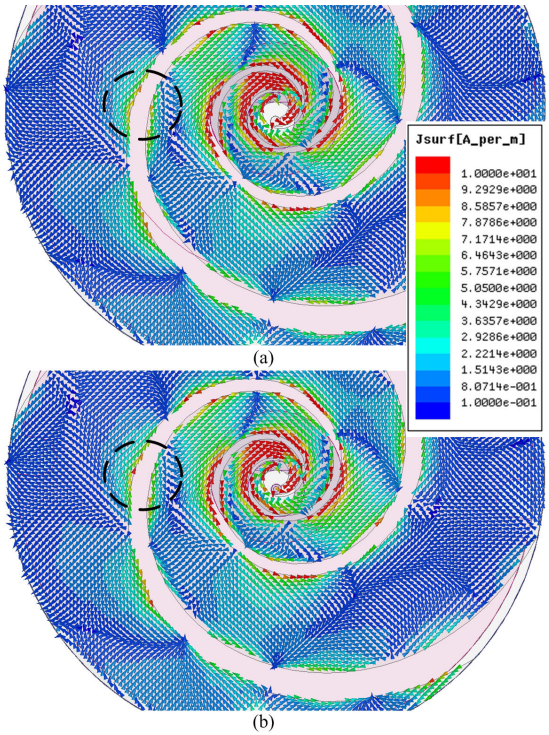

FIGURE 11. Current distributions of the antennas using (a) stepped cylindrical absorbing material and (b) ring-shaped absorbing material with $da2 = da1 = 109.6$ mm, $ha2 = 7$ mm at 5.8 GHz.

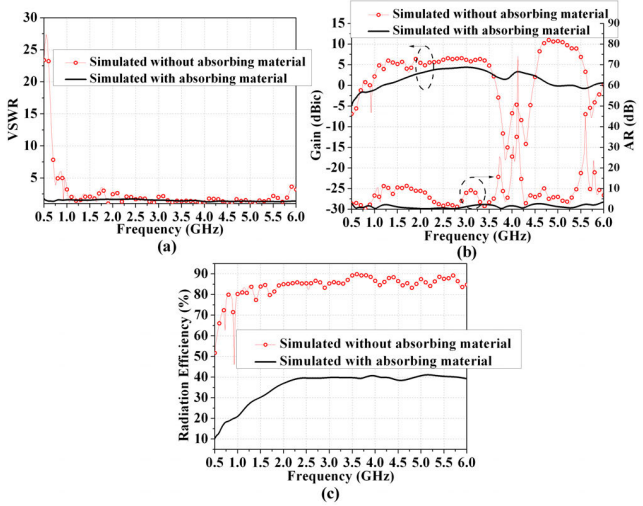

FIGURE 12. Simulated results with and without the absorbing material. (a) VSWR, (b) broadside gain and AR, and (c) radiation efficiency.

while in the high-frequency band, the radiation efficiency is approximately 40%.

IV. EXPERIMENTAL RESULTS

The proposed CP spiral antenna with a compact size of 113.6 mm × 39 mm (diameter × height, $0.189\lambda_{0.5\ \mathrm{GHz}} \times 0.065\lambda_{0.5\ \mathrm{GHz}}$) was fabricated. To ensure the stability of the structure, we wound a layer of fiberglass cloth around the z-directional helix. The radiation performance of the antenna was measured in an anechoic chamber (shown in Fig. 13).

FIGURE 13. Photograph of the fabricated antenna.

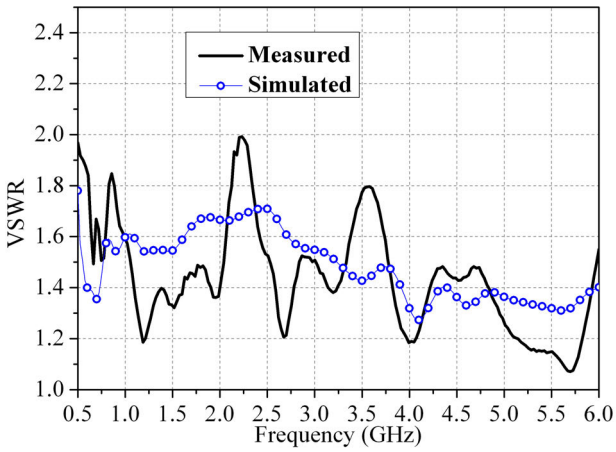

FIGURE 14. Measured and simulated VSWRs of the proposed antenna.

The simulated and measured VSWRs are depicted in Fig. 14. This discrepancy is mainly caused by the stepped cylindrical absorbing material, which was held together by glue, thereby affecting the electromagnetic parameters of the absorbing material. This cannot be included in the simulation. The measured impedance bandwidth for VSWR ≤ 2 is in the range of 0.5 to 6 GHz, with a fractional bandwidth of 169.2%. The measured and simulated results for the broadside gain and AR are shown in Fig. 15. The measured 3-dB AR bandwidth is from 0.5 to 5.8 GHz (168.3%). The measured minimum and maximum broadside gain are -5.3 and 4.6 dBic, respectively.

Fig. 16 shows the simulated and measured right-hand circular polarization (RHCP) radiation patterns. It can be observed that the unidirectional radiation properties of the

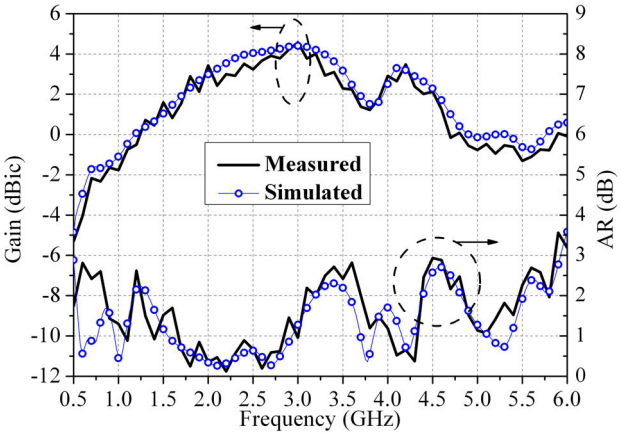

FIGURE 15. Measured and simulated results of the broadside gain and AR.

TABLE 2. Comparisons of proposed and other CP spiral antennas.

	Impedance bandwidth	3-dB AR bandwidth	Size	Gain (dBic)
[11]	3-10 GHz (107.7%) (VSWR ≤ 2)	AR > 3 dB (63.6% of measured frequencies)	$\phi 0.652\lambda_{3GHz} \times 0.1\lambda_{3GHz}$ (only spiral)	about 3.8~10.4
[12]	1.625-10 GHz (144.1%) (VSWR ≤ 2)	1.63-10 GHz (143.9%)	$\phi 0.348\lambda_{1.63GHz} \times 0.206\lambda_{1.63GHz}$	--
[13]	0.8-4.37 GHz (138.1%)	0.9-4.37 GHz (131.7%)	$0.3\lambda_{0.9GHz} \times 0.3\lambda_{0.9GHz} \times 0.15\lambda_{0.9GHz}$	7.5~13
[14]	0.8-3 GHz (115.8%) (VSWR ≤ 2)	AR > 3 dB in the band of 0.8- 1.95 GHz	$\phi 0.203\lambda_{0.8GHz} \times 0.102\lambda_{0.8GHz}$	about -10~5
[15]	3-4.8 GHz (VSWR > 2) 4.8-10 GHz (VSWR ≤ 2)	AR > 3 dB at frequencies 3 and 9 GHz	$\phi 0.6\lambda_{3GHz} \times 0.085\lambda_{3GHz}$	--
[16]	3-10 GHz (107.7%)	AR > 3 dB in the bands of 3-3.8 GHz and 5-5.4	$1.67\lambda_{3GHz} \times 1.67\lambda_{3GHz} \times 0.07\lambda_{3GHz}$	--
[17]	0.3-1 GHz (107.7%) (VSWR ≤ 2)	0.3-1 GHz (107.7%)	$0.4\lambda_{0.3GHz} \times 0.4\lambda_{0.3GHz} \times 0.061\lambda_{0.3GHz}$	about -5~6
[18]	0.5-1.4 GHz (94.7%) (VSWR ≤ 2.4)	0.5-1.4 GHz (94.7%)	$\phi 0.21\lambda_{0.5GHz} \times 0.09\lambda_{0.5GHz}$	-5~3.1
[19]	1.9-8.5 GHz (126.9%) (VSWR ≤ 2)	2-6 GHz (100%)	$\phi 0.24\lambda_{2GHz} \times 0.13\lambda_{2GHz}$	-6~7.5
Prop.	0.5-6 GHz (169.2%) (VSWR ≤ 2)	0.5-5.8 GHz (168.3%)	$\phi 0.189\lambda_{0.5GHz} \times 0.065\lambda_{0.5GHz}$	-5.3~4.6

patterns in the high-frequency band disappear due to the antenna height being too high.

The performance of the proposed antenna is compared to that of different CP spiral antennas studied in [11]–[19]; the comparison is presented in Table 2. The proposed antenna obtains better impedance and AR bandwidths, as well as a smaller overall size.

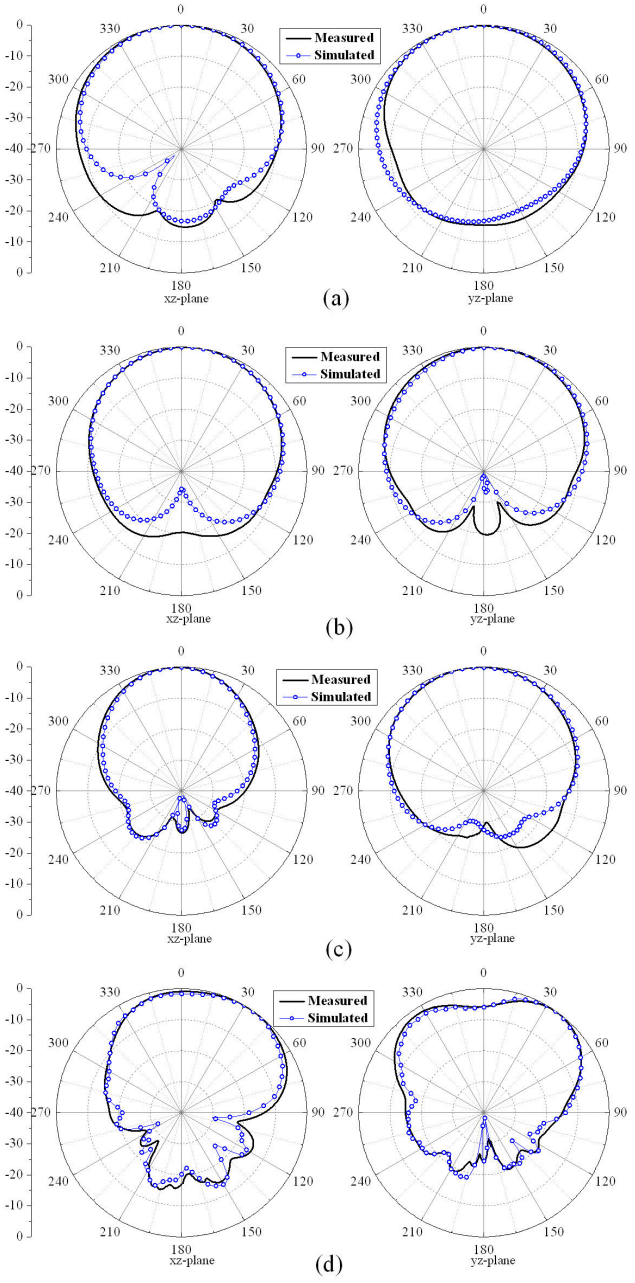

FIGURE 16. Radiation patterns of the two principal planes at (a) 0.5 GHz, (b) 1.5 GHz, (c) 3 GHz, and (d) 5.5 GHz.

V. CONCLUSION

A wideband CP spiral antenna fed by a tapered coax balun is presented. By using a nonself-complementarity spiral, a z-directional helix, and absorbing material with a stepped cylindrical honeycomb structure, the impedance and AR bandwidths are improved, and the overall size of the antenna is reduced. Experiments show that the antenna achieves a 169.2% impedance bandwidth for VSWR ≤ 2 and a 168.3% 3-dB AR bandwidth. The antenna has a small size of 113.6 mm × 39 mm ($0.189\lambda_{0.5\ GHz} \times 0.065\lambda_{0.5\ GHz}$).

REFERENCES

[1] N. Rahman and M. N. Afsar, "A novel modified archimedean polygonal spiral antenna," *IEEE Trans. Antennas Propag.*, vol. 61, no. 1, pp. 54–61, Jan. 2013.

[2] T.-K. Chen and G. H. Huff, "Stripline-fed archimedean spiral antenna," *IEEE Antennas Wireless Propag. Lett.*, vol. 10, pp. 346–349, 2011.

[3] S.-G. Mao, J.-C. Yeh, and S.-L. Chen, "Ultrawideband circularly polarized spiral antenna using integrated balun with application to time-domain target detection," *IEEE Trans. Antennas Propag.*, vol. 57, no. 7, pp. 1914–1920, Jul. 2009.

[4] W. Fu, E. R. Lopez, W. S. T. Rowe, and K. Ghorbani, "A planar dual-arm equiangular spiral antenna," *IEEE Trans. Antennas Propag.*, vol. 58, no. 5, pp. 1775–1779, May 2010.

[5] P. H. Rao, M. Sreenivasan, and L. Naragani, "Dual band planar spiral feed backed by a stepped ground plane cavity for satellite boresight reference antenna applications," *IEEE Trans. Antennas Propag.*, vol. 57, no. 12, pp. 3752–3756, Dec. 2009.

[6] H. Nakano, K. Kikkawa, Y. Iitsuka, and J. Yamauchi, "Equiangular spiral antenna backed by a shallow cavity with absorbing strips," *IEEE Trans. Antennas Propag.*, vol. 56, no. 8, pp. 2742–2747, Aug. 2008.

[7] J. R. Mruk, Y. Saito, K. Kim, M. Radway, and D. S. Filipovic, "Directly fed millimetre-wave two-arm spiral antenna," *Electron. Lett.*, vol. 46, no. 24, pp. 1585–1587, Nov. 2010.

[8] H. Nakano, R. Satake, and J. Yamauchi, "Extremely low-profile, single-arm, wideband spiral antenna radiating a circularly polarized wave," *IEEE Trans. Antennas Propag.*, vol. 58, no. 5, pp. 1511–1520, May 2010.

[9] N. Ghassemi, K. Wu, S. Claude, X. Zhang, and J. Bornemann, "Compact coplanar waveguide spiral antenna with circular polarization for wideband applications," *IEEE Antennas Wireless Propag. Lett.*, vol. 10, pp. 666–669, 2011.

[10] S. Mohamad, R. Cahill, and V. Fusco, "Performance of archimedean spiral antenna backed by FSS reflector," *Electron. Lett.*, vol. 51, no. 1, pp. 14–16, Jan. 2015.

[11] M. Veysi and M. Kamyab, "Bandwidth enhancement of low-profile PEC-backed equiangular spiral antennas incorporating metallic posts," *IEEE Trans. Antennas Propag.*, vol. 59, no. 11, pp. 4315–4318, Nov. 2011.

[12] Y.-W. Wang, G.-M. Wang, and H.-Y. Zeng, "Design of a new meander archimedean spiral antenna," *Microw. Opt. Technol. Lett.*, vol. 52, no. 10, pp. 2384–2387, Jul. 2010.

[13] S. M. H. Ranjbaran and S. Mohanna, "Improved spiral antenna with a new semi-fractal reflector for short-range sensing," *IET Microw., Antennas Propag.*, vol. 12, no. 11, pp. 1839–1845, Sep. 2018.

[14] J. M. O'Brien, J. E. Grandfield, G. Mumcu, and T. M. Weller, "Miniaturization of a spiral antenna using periodic Z-plane meandering," *IEEE Trans. Antennas Propag.*, vol. 63, no. 4, pp. 1843–1848, Apr. 2015.

[15] S. Mohamad, R. Cahill, and V. Fusco, "Selective high impedance surface active region loading of archimedean spiral antenna," *IEEE Antennas Wireless Propag. Lett.*, vol. 13, pp. 810–813, 2014.

[16] H. Nakano, K. Kikkawa, N. Kondo, Y. Iitsuka, and J. Yamauchi, "Low-profile equiangular spiral antenna backed by an EBG reflector," *IEEE Trans. Antennas Propag.*, vol. 57, no. 5, pp. 1309–1318, May 2009.

[17] M. Tanabe, Y. Masuda, and H. Nakano, "Low-profile spiral antenna placed on an extremely thin magnetodielectric substrate," *IEEE Antennas Wireless Propag. Lett.*, vol. 16, pp. 2050–2053, 2017.

[18] T.-Y. Shih and N. Behdad, "A compact, broadband spiral antenna with unidirectional circularly polarized radiation patterns," *IEEE Trans. Antennas Propag.*, vol. 63, no. 6, pp. 2776–2781, Jun. 2015.

[19] Y.-W. Zhong, G.-M. Yang, J.-Y. Mo, and L.-R. Zheng, "Compact circularly polarized archimedean spiral antenna for ultrawideband communication applications," *IEEE Antennas Wireless Propag. Lett.*, vol. 16, pp. 129–132, 2017.

LING-LU CHEN was born in China, in 1986. She received the B.S. degree in electronic science and technology and the Ph.D. degree in electromagnetic field and microwave technology from Southwest Jiaotong University, Chengdu, China, in 2008 and 2014, respectively.

She joined the No. 36 Research Institute, CETC, in 2014, where she is currently a Senior Engineer. Her recent research interest includes UWB antenna and array.

LEI CHANG was born in China, in 1986. He received the B.S. degree in electronic science and technology and the Ph.D. degree in electromagnetic field and microwave technology from Southwest Jiaotong University, Chengdu, China, in 2007 and 2013, respectively.

He joined the No. 36 Research Institute, CETC, in 2013, where he is currently a Senior Engineer. His recent research interests include UWB antenna and millimeter-wave antenna.

ZHUANG-ZHI CHEN was born in China, in 1986. He received the B.S. degree in electronic and information engineering from Xidian University, Xi'an, China, in 2008.

He joined the No. 36 Research Institute, CETC, in 2008, where he is currently a Senior Engineer. His recent research interests include UWB antenna and direction finding antenna design.

QIAO-NA QIU was born in China, in 1989. She received the B.S. degree in electronic and information and the M.S. degree in electromagnetic field and microwave technology from Xidian University, Xi'an, China, in 2011 and 2014, respectively.

She joined the No. 36 Research Institute, CETC, in 2014, where she is currently an Engineer. Her recent research interest is UWB antenna design.